Ground Water Monitoring & Remediation

Pore Water Characteristics Following a Release of Neat Ethanol onto Pre-existing NAPL

by Brent P. Stafford, Natalie L. Cápiro, Pedro J.J. Alvarez, and William G. Rixey

Abstract

Neat ethanol (75.7 L) was released into the upper capillary zone in a continuous-flow, sand-packed aquifer tank (8.2 m^3) with an average seepage velocity of 0.75 m/day. This model aquifer system contained a residual nonaqueous phase liquid (NAPL) that extended from the capillary zone to 10 cm below the water table. Maximum aqueous concentrations of ethanol were 20% v/v in the capillary zone and 0.08% in the saturated zone at 25 and 30 cm downgradient from the emplaced NAPL source, respectively. A bench-scale release experiment was also conducted for a similar size spill (scaled to the plan area). The concentrations of ethanol in ground water for both the bench- and pilot-scale experiments were consistent with advective–dispersive limited mass transfer from the capillary to the saturated zone. Concentrations of monoaromatic hydrocarbons and isooctane increased in the pore water of the capillary zone as a result of both redistribution of residual NAPL (confirmed by visualization) and enhanced hydrocarbon dissolution due to the cosolvent effect exerted by ethanol. In the tank experiment, higher hydrocarbon concentrations in ground water were also attributed to decreased hydrocarbon biodegradation activity caused by preferential microbial utilization of ethanol and the resulting depletion of oxygen. These results infer that spills of highly concentrated ethanol will be largely confined to the capillary zone due to its buoyancy, and ethanol concentrations in near-source zone ground water will be controlled by mass transfer limitations and hydrologic conditions. Furthermore, highly concentrated ethanol releases onto pre-existing NAPL will likely exacerbate impacts to ground water, due to NAPL mobilization and dissolution, and decreased bioattenuation of hydrocarbons.

Introduction

Concerns regarding potential ground water impacts from spills of highly concentrated ethanol have arisen due to the recent increase in use and transport of higher ethanol content fuel blends. Likely release scenarios include E85 (85% ethanol; 15% gasoline v/v) leaking from underground storage tanks at service stations and fuel grade (denatured) ethanol (95% ethanol; 5% gasoline) spills during transport or after reaching bulk terminals. Although some attention has been given to the impacts of ethanol on the natural attenuation of benzene, toluene, and xylenes (BTX) plumes (Powers et al. 2001a,b; da Silva and Alvarez 2002; Deeb et al. 2002; Molson et al. 2002; MacKay et al. 2006), little is known about how physical–chemical processes influence the concentration of hydrocarbons in pore water near a source of a fuel ethanol spill.

The cosolvent effect of ethanol on hydrocarbons has been shown in laboratory (Heermann and Powers 1998; Rixey and He 2001; Corseuil et al. 2004), modeling (Powers et al. 2001a; Deeb et al. 2002; Molson et al. 2002; Gomez et al. 2008) and field investigations where ethanol was used as a remediation agent (Rao et al. 1997). There have also been reported investigations of accidental fuel ethanol (E95) releases (McDowell et al. 2003) as well as controlled spills of ethanol at field sites (Molson et al. 2008). In addition, laboratory studies have shown how ethanol blend releases behave and influence hydrocarbon migration in the unsaturated and capillary zones (Jawitz et al. 1998; McDowell and Powers 2003; McDowell et al. 2003; Lee 2008), and how fluid flows and solutes migrate in the capillary fringe (Silliman et al. 2002; Abit et al. 2008). A recent pilot-scale investigation linked a release of fuel grade ethanol to concentrations of ethanol and hydrocarbons in ground water near the source, and found that ethanol movement is confined to the capillary zone, significantly limiting the extent of the impact to ground water (Cápiro et al. 2007). These studies have improved our understanding of the physical behavior of fuel ethanol components in the subsurface. However, quantitative studies of the effect of ethanol releases onto pre-existing hydrocarbon contamination are lacking, and the transfer of ethanol and hydrocarbons from the capillary zone to ground water remains poorly understood.

This study evaluated ground water impacts from a spill of neat ethanol near pre-existing residual NAPL. Pilot- and

bench-scale experiments were used to couple analysis of soil and pore water ethanol and hydrocarbon concentrations (and associated mass transfer from the capillary zone) with qualitative visualization of ethanol and NAPL movement. Capillary and saturated zone pore water concentrations of ethanol and hydrocarbons were monitored in both systems to obtain a more complete assessment of the physical–chemical behavior of fuel ethanol releases near pre-existing NAPL.

Materials

Porous Media

Two fine-grained sands were used for the experiments: southeast Texas sand (Circle Sand; Houston, Texas) and Ottawa-Federal Fine™ (U.S. Silica; Ottawa, Illinois). Ottawa sand, which is lighter in color, was used for the bench-scale release to enhance visualization of the capillary zone and also for better definition of the two dyes used to track the migration of NAPL and ethanol (hydrophobic Sudan-IV and hydrophilic Fluorescein, respectively). The two sand types have similar particle size distributions (Table 1) and capillary zone heights (Table 2). The S.E. Texas sand was used for the pilot-scale release because of cost considerations.

Table 1
Media Properties

Analysis	Ottawa Federal-Fine (US Silica)	S.E. Texas (Circle Sand Inc.)
pH	7	6.8
Organic matter	< .01%	0.09%
D_{50}	0.3 mm	0.2 mm
D_{60}/D_{10}	1.67	1.70

Chemicals

The composition of the NAPL mixture was benzene (2.0% by weight), toluene (5.6%), m-xylene (11.7%), 1,2,4 trimethylbenzene (TMB) (29.4%), and isooctane (51.3%). All of the NAPL components were obtained from Sigma Aldrich (Milwaukee, Wisconsin). The same NAPL composition and neat ethanol (anhydrous, AAPER Alcohol and Chemical Co., Shelbyville, Kentucky) were used for both experiments. Neat ethanol was used instead of denatured ethanol to avoid interference of denaturants with pre-existing NAPL components. Three dyes were used: Sudan-IV (Sigma-Aldrich), a hydrophobic dye, was added at 100 mg/L to the NAPL, and Fluorescein (Sigma Aldrich), a hydrophilic dye, was added as a free acid to the neat ethanol at 100 mg/L. Diluted propylene glycol was also used as a dye tracer in the bench-scale experiment to determine flow paths using methods similar to those in Silliman et al. (2002). Dissolved sodium bromide (10 g/L) and calcium chloride (5 g/L) were used as conservative tracers in the pilot-scale and bench-scale experiments, respectively.

Methods

Experimental Systems

A bench-scale release of neat ethanol near residual NAPL was conducted in a continuous-flow, sand-packed, glass 2D cell (Figure 1). Prepurified deionized (DI) water

Table 2
Bench- and Pilot-Scale Experimental Conditions

	Bench Scale	Pilot Scale
System		
System volume (m^3)	0.01	8.2
Sand type	Ott. Federal Fine	S.E. Texas sand
Capillary zone height (cm)	24 ± 1	25 ± 2
Sat. zone height (m)	0.15	0.74
Flow rate (mL/min)	0.05	300 to 400
Sat. zone seepage velocity(1) (cm/day)	3	75
Temperature (°C)	24	25 to 40
Monitoring duration (days)	485	100
Source zone		
LNAPL volume (L)	0.044	5.8
Source zone volume (m^3)	0.0013	0.165
NAPL saturation ($cm^3_{NAPL}/cm^3_{pore\ space}$)	0.1	0.1
Ethanol release		
Vol. EtOH released (L)	0.8	75.7
EtOH injection rate (mL/min)	6	210
VOL_{ETOH}/A(2) (cm)	3.2	2.5

(1)Average velocity not including temporary influences of tracer and ethanol loadings.

(2)A = plan view area of emplaced NAPL source.

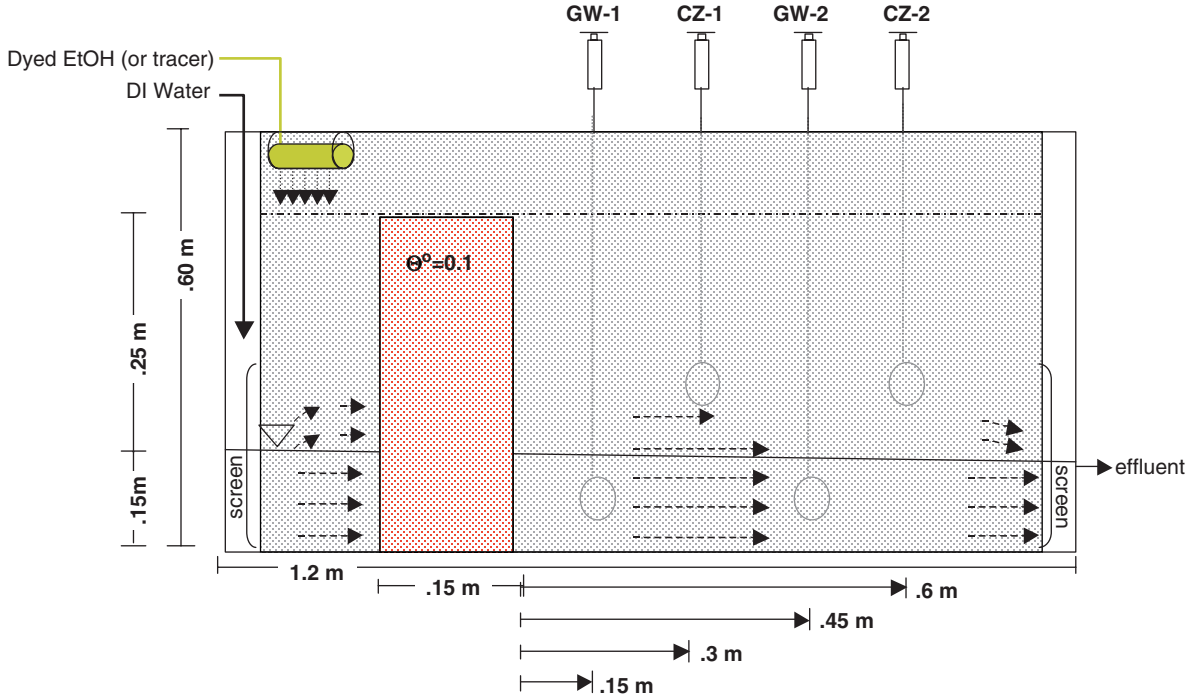

Figure 1. Two-dimensional cell experimental design for a bench-scale release of 0.8 L of E100 onto residual NAPL. Dashed arrows represent flow paths in the saturated and capillary zone (confirmed by spot dye injections). Samples were collected above and below the water table (open circles), in the outlet well, and from the effluent.

was fed to the cell at a continuous flow rate of 0.05 mL/min using a Masterflex pump model # 7520 (Cole-Parmer, Vernon Hills, Illinois). Before emplacement of the NAPL source, the glass-walled cell was packed with clean sand in 2 cm lifts and kept separated from the source region by temporary acrylic retaining walls. Each lift was evenly spread, followed by manual compaction as the cell was slowly filled with water, but the sand surface was not submerged. After packing, the water level was raised above the sand surface to prevent the accumulation of trapped air. The cell was subsequently drained to field capacity. The residual NAPL source was created by mixing the NAPL containing 100 mg/L Sudan-IV with wet sand in a 10 × 15 cm air-tight plastic bag (Minigrip) to obtain a NAPL saturation of 0.1 cm^3 NAPL/cm^3 pore space (Table 2). Immediately following the mixing, the contaminated sand was emplaced by packing 2 cm lifts from the bottom of the cell to the top of the capillary zone and packing additional clean sand on top (Figure 1). As the source was being packed, the temporary retaining walls were slowly removed and the newly emplaced contaminated sand was packed tightly against the clean sand. Following source emplacement, the system was drained to a water table level of 15 cm and subsequently ran continuously for 15 days before the introduction of ethanol in order to conduct tracer tests and to achieve a stable dissolved hydrocarbon plume downgradient of the emplaced source.

Similarly, a pilot-scale release of neat ethanol near preexisting residual NAPL was conducted in a continuous-flow, sand-packed aquifer tank (Figure 2). Municipal (Houston, Texas) tap water with a measured pH of 7.5 ± 0.4, dissolved oxygen concentration of 3 mg/L, and an ionic strength of 6 to 12 mM was continuously fed to the tank at a rate of 300 to 400 mL/min. This was the minimum flow rate necessary to maintain continuous and stable flow for the hydraulic configuration of the tank.

The tank was packed with sand similar to methods previously described (Cápiro et al. 2007) and subsequently drained to the target water table level (0.74 m). The residual NAPL source (Table 2) was created in a manner similar to the bench-scale method with larger bags (36 × 61 cm). Each bag contained 10 kg of wet sand mixed with 250 mL NAPL. The contaminated sand was then immediately packed in 5 cm lifts into an excavated trench with temporary barriers to create the source zone, followed by packing tightly against the adjacent clean sand and emplacement of additional clean sand on top of the source. The system then ran for 18 days before the introduction of ethanol in order to achieve stable hydrocarbon concentrations downgradient of the emplaced source. The biodegradation potential was assessed by quantifying microbial populations harboring the aerobic catabolic genes *dmpN* (coding for phenol hydroxylase) and *todC1* (coding for toluene dioxygenase), both known to be associated with BTX degradation. Full details regarding the microbial analysis can be found elsewhere (Cápiro et al. 2008).

The flow rate for the bench-scale experiment was deliberately lower than that for the pilot-scale experiment (Table 2) to yield higher concentrations in the saturated zone. In both experiments, samples were taken from the capillary and saturated zones and the effluent for analysis of gasoline hydrocarbons and ethanol pore water concentrations, and for mass balance calculations at different locations throughout the systems.

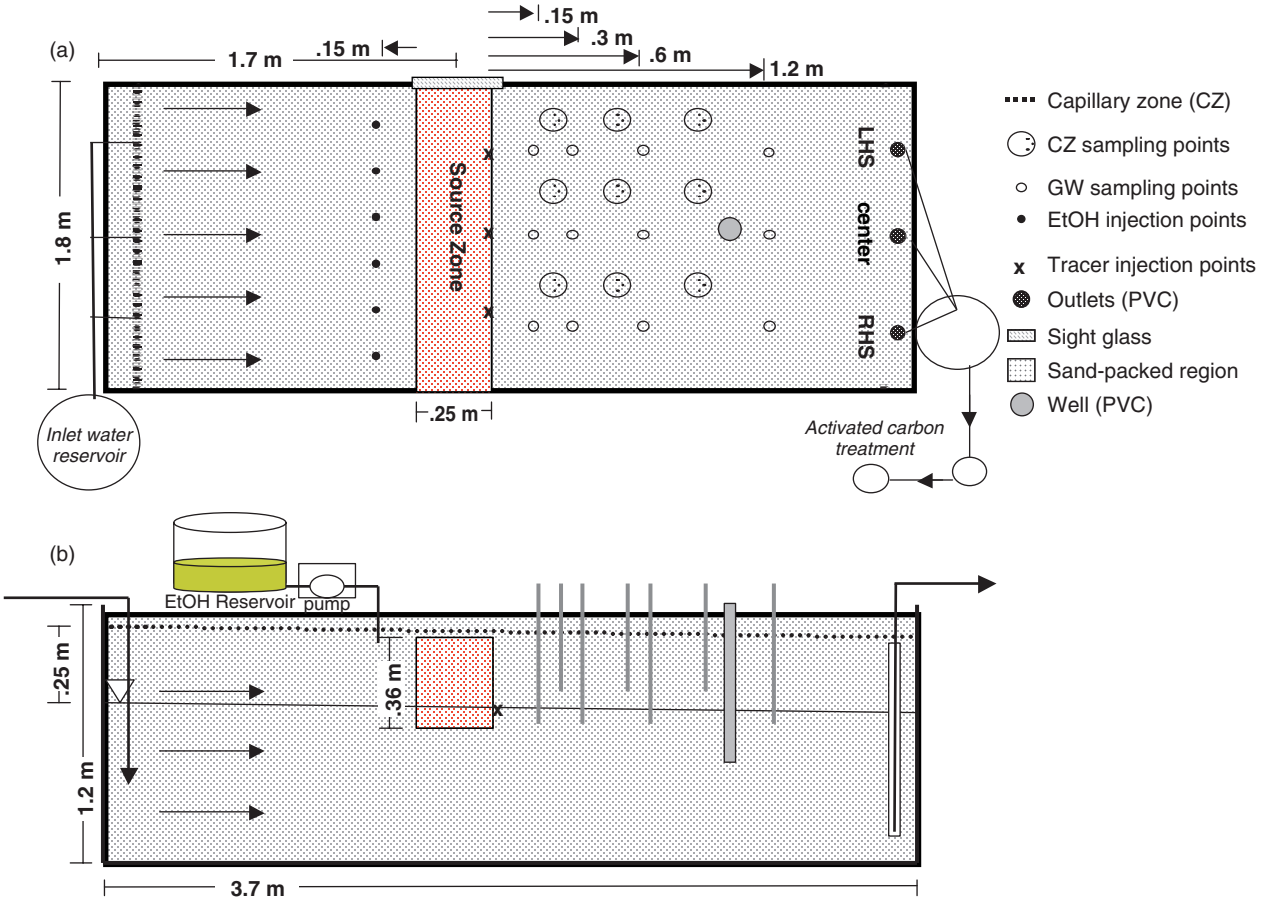

Figure 2. (a) Plan view and (b) profile view of the pilot-scale release experimental design. The pattern-shaded rectangles represent the emplaced source and the dotted line represents the initial capillary zone height.

Hydraulic Characterization

Bench Scale

Injections of 1 mL of diluted propylene glycol dye (25% v/v) were made at several locations to determine saturated and capillary zone flow paths and seepage velocities. Spot tracer methods for estimating capillary zone seepage velocities were adapted from Silliman et al. (2002). Ten days into the experiment, 800 mL of a tracer solution (approximately 5 g/L $CaCl_2$) was added to the system 30 cm above the water table and 10 cm upgradient of the emplaced source (Figure 1) at 6 mL/min to determine the hydraulic characteristics in the cell before the ethanol release and to compare retention of a spill of ethanol in the system with an equivalent volume of water. Tracer samples (1 mL) were collected with a 20 gauge needle (Popper and Sons Inc., New Hyde Park, New York) pushed down to the desired sampling depth. Samples were prepared and analyzed by diluting (1:3) with DI water and using a salinity probe (American Marine, Ridgefield, Connecticut). For the first 10 days of the experiment, the water table gradient was maintained at 0.01 m/m and the seepage velocity in the saturated zone (determined by the spot dye tracers) was 2 to 3 cm/day. The seepage velocity at 8 cm above the water table (1/3 of the capillary zone) was approximately 1 cm/day. After the chloride tracer solution was added, the groundwater velocity increased to a maximum of 30 cm/day. Five days following the tracer release (15 days after the source was emplaced), the gradient and seepage velocity returned to pretracer levels of 0.01 m/m and 3 cm/day.

Pilot Scale

Before the emplacement of the source, 75.7 L of a 10 g/L bromide tracer solution was injected into the system to determine the hydraulic conditions within the sampling region of the tank (Figure 2). The tracer solution was injected into the tank at 210 mL/min from three Peristaltic Masterflex pumps (Easy-load L/S Cole-Parmer 7518-10, Vernon Hills, Illinois) with Viton tubing connected by hose clamps to 0.64 cm (1/4 inch) stainless steel tubing with the open ends located at three injection points evenly distributed along the width of the tank. The total time for injection was 6 h. Injection points were located at the water table at the same position as the downgradient edge of the emplaced NAPL source. Bromide samples were collected in 125 mL HDPE field sampling bottles (Fisher Scientific; Pittsburgh, Pennsylvania) and analyzed using a bromide ion selective electrode (Cole-Parmer) using methods described in Cápiro et al. (2007). Breakthrough data indicated a seepage velocity of 0.6 to 0.9 m/day and a hydraulic conductivity of 0.02 to 0.03 cm/s.

Neat Ethanol (E100) Release

Bench Scale

Fifteen days following the emplacement of the NAPL source, neat ethanol (800 mL) was released to the system at the same location (Figure 1) and under conditions similar to the tracer release (Table 2). On day 398, a simulated recharge event was conducted by introducing 4.5 L of DI water evenly at the sand surface to flush any remaining ethanol from the unsaturated zone.

Pilot Scale

Eighteen days following the emplacement of the NAPL source, neat ethanol (75.7 L) was introduced near the top of the capillary zone and 15 cm behind the upgradient edge of the emplaced source (Figure 2b). The ethanol solution was introduced at a rate of 210 mL/min from six equally spaced injection points using six Masterflex pumps over 6 h. The spill volume to surface area ratio of the experimental region and the NAPL volumes (as a fraction of total pore volume) were similar to that for the bench-scale release (Table 2).

Sampling

Bench Scale

More than 500 saturated zone, capillary zone, and effluent samples were collected throughout the experiment and analyzed for hydrocarbons and ethanol. Saturated and capillary zone samples were collected using 12 inch, 20 gauge, deflected point needles (Popper & Sons, New Hyde Park, New York) connected to 3 mL plastic syringes (BD Biosciences, San Jose, California). Effluent samples were collected from the outlet well within the top 1 cm and at the midpoint of the well height (7.5 cm) using a syringe and a 20 gauge needle. Approximately 2.1 mL was collected at each sampling point and transferred to a 2 mL glass vial (Sun SRI; Duluth, Georgia) and stored at 4°C before analysis.

On day 485, porous media samples (5 g) were obtained after removal of the front glass wall. The samples were placed into 43 mL glass vials (VWR International; West Chester, Pennsylvania) and prepared and analyzed according to methods described below.

Pilot Scale

More than 1000 saturated zone, capillary zone, and outlet samples were analyzed for gasoline hydrocarbons and ethanol. Aqueous samples were collected until ethanol concentrations in the effluent were below the method detection limit (10 mg/L). Sampling locations are shown in Figures 2a and 2b. Saturated zone (3 cm below the water table) and effluent samples were collected using 60 mL plastic syringes (Fisher Scientific). This was accomplished by first drawing out and disposing 1.5 line volumes, then collecting 43 to 45 mL into gas-tight 43 mL glass vials (VWR) without headspace, followed by storage at 4°C. Capillary zone samples were collected using a 12 inch, 20 gauge deflected point needles (Popper & Sons) connected to a 3 mL plastic syringe (BD). Approximately 2.5 mL was collected at each capillary zone sampling point. To obtain a greater sampling volume and avoid pulling water from below the water table, capillary zone samples from three closely spaced sampling points (less than 3 cm spacing) in a triangular pattern (enclosed in a 15 cm diameter PVC ring for reference) were collected and analyzed to obtain an average concentration in that region (Figure 2a). Two milliliters of each capillary zone sample was transferred to a gas-tight 2 mL vial (Sun SRI) followed by storage at 4°C before analysis. In addition to aqueous sampling for hydrocarbon and ethanol, 25 mL samples were also collected from selected saturated zone sampling points (at 3 cm below the water table) for measurement of dissolved oxygen.

Sand cores were collected using 5 cm in diameter HDPE cylinders (GSI Environmental, Houston, Texas) with retaining caps hammered in from the surface to the targeted depth and stored at 0°C before analysis.

Analytical Methods

Aqueous Analyses

Aqueous samples were centrifuged at 2000 rpm for 5 min, and supernatant was collected in 2 mL gas-tight glass vials with polypropylene caps and PTFE septa (Sun SRI). The concentrations of BTX, TMB, isooctane, and low concentrations of ethanol (up to 10% v/v) were measured by direct aqueous injection on a Hewlett Packard model 6890 gas chromatograph equipped with a Supelco capillary column model SPB-5 (30 m length, 0.53 mm diameter, 5 μm film thickness) and an OI Analytical flame ionization detector (OI Analytical; College Station, Texas). Practical quantitation limits (PQLs) were nominally 1 mg/L for each gasoline hydrocarbon compound. This relatively high PQL was adequate for the scope of the studies, and the direct injection method allowed for timely analyses of the high number of samples associated with the pilot-scale experiment.

Analysis of higher concentrations of ethanol (above 10% v/v) was done gravimetrically. A calibration curve was generated using five targeted concentrations of ethanol in 2 mL ethanol + DI water solutions suspended in an isothermal bath. Sample density was obtained by averaging the weights of three 0.5 mL volumes.

For the pilot-scale experiment, dissolved oxygen was measured using CHEMets Kits K-7512 (1 to 12 mg/L) and K-7501(0 to 1 mg/L) (CHEMetrics; Calverton, Virginia).

Media Analyses

Sand cores were analyzed for moisture content, ethanol, and BTX, TMB, and isooctane concentrations. For the extractions conducted in the bench-scale experiment, 5 g of media were placed directly into a 43 mL glass vial (VWR). For the pilot-scale experiments, samples were prepared by dividing each core into 10.2 cm vertical segments with an approximate volume of 200 cm^3 and homogenizing them. Five grams of the sample were then placed into a 43 mL glass vial. In both cases, the vials were then filled (no headspace) with HPLC grade methanol (Sigma Aldrich) (for extraction of gasoline hydrocarbons) or with DI water (for extraction of ethanol) and manually shaken. Extractions

were conducted in triplicate. Quantitative recoveries for all compounds except isooctane were achieved. For isooctane, two successive methanol extractions were used. The recoveries for spiked soil samples ranged from 70% to 90%.

Before analysis, the sand core extractions were centrifuged at 2000 rpm for 5 min, and supernatant was collected into 2 mL gas-tight glass vials with HDPE caps and PTFE septa (Sun SRI). Supernatant analysis was conducted according to the aqueous sample methods described previously. Moisture contents were determined by drying 10 g of soil in glass vials covered with aluminum foil at 200°C for 8 h and measuring the loss of mass. Analyses for moisture content and ethanol and fuel components were done in duplicate.

Results and Discussion

Visualization

Bench Scale

A time-series of photographs are presented as Figure 3. Ethanol was released near the top of the capillary zone and 10 cm upgradient from the emplaced source edge. This configuration yielded a relatively short-term source of ethanol upstream of the NAPL source zone as some ethanol became temporarily trapped from the nonhorizontal flow in the capillary zone at the upgradient edge of the cell (Figure 3a). As the released ethanol encountered the source zone, residual NAPL in the ethanol path was quickly dissolved and removed by the advancing ethanol front (Figure 3b). The bulk fuel (EtOH + dissolved NAPL) then moved downgradient from the source in the capillary zone with a wedge-shaped leading edge similar to that described in previous capillary zone surface-tension driven flow (Henry and Smith 2002) and ethanol flushing (Jawitz et al. 1998; Grubb and Sitar 1999) studies.

As evident by the position of the Fluorescein dye, the ethanol behind the advancing front temporarily built up above the water table and upgradient of the source. This temporarily increased the hydraulic head and caused some ethanol to be pushed just below the initial water table. However, ethanol returned to its position above the water table within 24 h, following its injection.

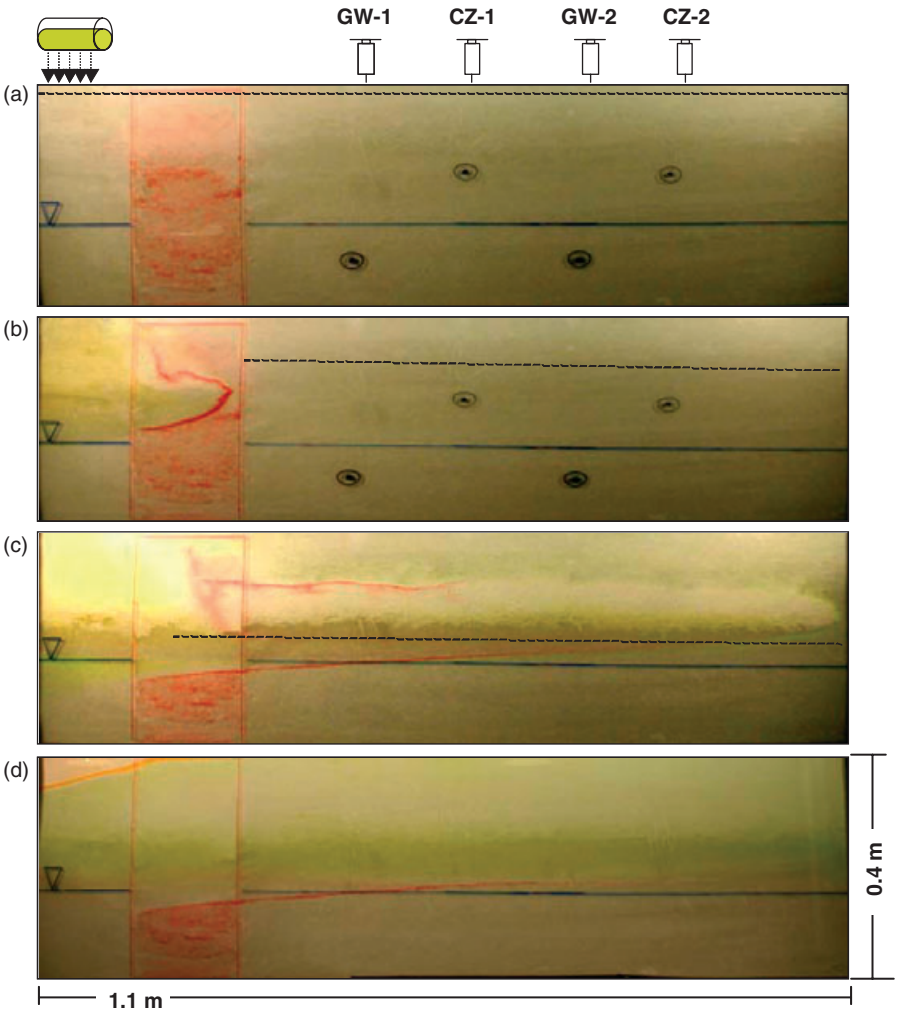

Figure 3. Flushing and redistribution of residual NAPL following the release of E100 in a bench-scale experiment. Red corresponds with the Sudan-IV dyed NAPL phase and bright yellow corresponds with Fluorescein-dyed concentrated ethanol (a) 15 days following the emplacement of the source and 5 days following the introduction of the tracer. (b) 1.5 h into the ethanol injection showing the ethanol front dissolving NAPL in its path. (c) 12 h following the start of the ethanol injection. (d) 100 days following the EtOH release (the orange line in the upper left corner is precipitated Fluorescein at the initial capillary fringe–air interface).

Ethanol moved predominantly horizontally through the system (approximately 1 m) in just over 12 h (compared with 4 days for the tracer), leaving a trail of phase-separated (redistributed) NAPL both just above and just below the ethanol path. The NAPL lens generated just below the path extended over a significantly longer distance than the generated NAPL lens above the path (Figure 3c). This corresponds to the greater degree of phase separation expected as fuel encounters higher water saturations closer to the water table, which decreases the cosolvent effect of ethanol (French and Malone 2005). However, the upper lens was flushed and removed within 24 h by the highly concentrated ethanol that passed behind the initial front and under the influence of a greater hydraulic gradient. The lower lens appeared to remain mostly undisturbed for the rest of the experiment (Figure 3d shows the NAPL lens condition at day 100).

Rapid drainage occurred in the region of the capillary zone just above the ethanol path behind the leading edge of the ethanol front. A new capillary zone height was reestablished at 11 cm within 5 days of the release—a 56% drop from the initial height. This corresponds to a reduction in surface tension from 72 dynes/cm to approximately 32 dynes/cm, which would indicate an ethanol concentration of 40% v/v (Lide 2005). This is consistent with measurements of capillary zone ethanol concentrations (discussed subsequently). As the ethanol continued to distribute within the pore water of the capillary zone, the height of the zone dropped and the hydraulic head (measured in the inlet well) increased. Recovery of the capillary zone height was observed to begin once peak levels of ethanol were reduced below 25% v/v; however, complete recovery was not obtained until after the simulated recharge event (day 398) when ethanol (and hydrocarbon) concentrations were reduced to below the PQLs (not shown). Although the capillary zone height would be expected to recover as ethanol dissipates (McDowell and Powers 2003), this study shows that complete recovery may not occur rapidly in the absence of surface recharge. Recovery of the capillary height would be expected to occur more rapidly in areas with a fluctuating water table. However, previous research has indicated that most of the highly concentrated ethanol in the capillary fringe tends to rise and fall along with a slowly fluctuating water table, consequently limited mixing occurs (Stafford 2007).

Below the water table, the NAPL source was mostly undisturbed except for a small thin section near the water table (Figure 3c) that was swept out by the fraction of ethanol initially held below the water table. The emplaced NAPL below the water table appeared to remain undisturbed over the 485-day monitoring period (Figure 3d).

Ethanol and Hydrocarbon Recovery

Bench Scale

Ethanol recovery was 92% after accounting for the mass associated with pore water samples drawn from the cell (Table 3). Compared with the tracer that flushed out of the system within 5.5 days, some ethanol remained in the system for nearly 400 days, at which time the simulated recharge event flushed the remaining ethanol from pore water above the water table (Figure 4a). This result is consistent with confinement of ethanol to the capillary zone (Figure 3) and is similar to that reported by others (McDowell et al. 2003; Cápiro et al. 2007).

Recoveries of hydrocarbon components were determined using the effluent flow rate and average concentrations above and below the water table at the furthest sampling cross sections (GW-2 and CZ-2 in Figure 1). Results from the effluent recovery analysis are presented in Table 3 along with mass associated with the soil cores as well as that associated with the pore water sampling. Recoveries of m-xylene and TMB were 119% and 84%, respectively. Mass recoveries for benzene, toluene, and isooctane were 15%, 62%, and 68%, respectively. The higher than 100% measured recovery for

Table 3
Mass Recovery in the Bench-Scale Experiment

	Ethanol (%)	*m*-Xylene (%)	TMB (%)
Effluent	87	119	84
Undisturbed residual source[1]	0	3	24
Redistributed LNAPL outside of source[1]	0	6	7
Removed during sampling	5.5	0.3	0.2
Total calculated recovery	92	128	115

[1]Calculated from average soil concentration.

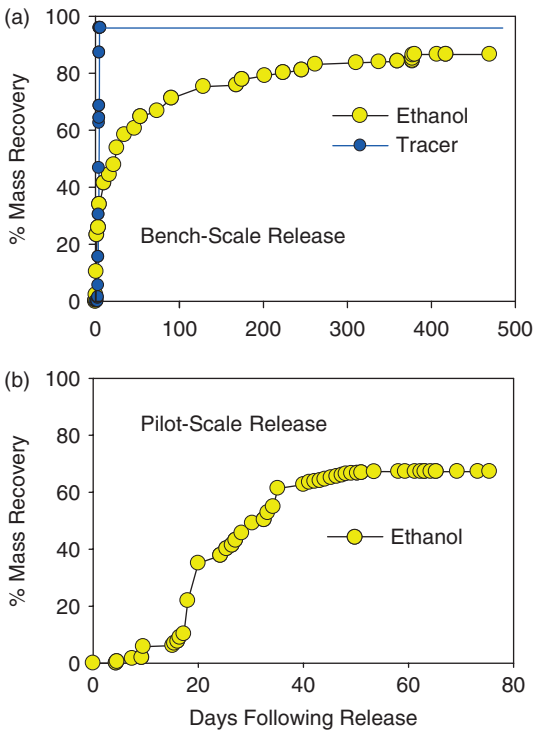

Figure 4. Effluent cumulative ethanol and tracer recoveries, (a) bench scale and (b) pilot scale.

m-xylene may be because of recoveries based on pore water concentration measurements in only two sample points: one in the saturated zone and the other in the unsaturated zone. The mass distribution results are not shown for benzene and toluene because of volatilization during packing of the NAPL that was not quantified and for isooctane because of incomplete extraction from soil samples by methanol. Mass distributions for m-xylene and trimethylbenzene (Table 3) support the visualization results, showing that a significant amount of NAPL was mobilized and redistributed.

For the soil cores, samples were collected from within the undisturbed source zone, the redistributed NAPL lens at the water table, and at several other points both above and below the water table. The thin NAPL lens, extending from the upper boundary of the remaining initial NAPL source to 0.6 m downgradient (Figure 3c), had total hydrocarbon concentrations as high as 10,300 mg/kg, with levels decreasing with distance from the source. Hydrocarbon concentrations were below the method detection limit (less than 10 mg/kg) at all other locations downstream of the source. Detailed soil concentration data can be found in Stafford (2007).

Pilot Scale

The peak ethanol concentration observed in the effluent was 5 g/L (0.6 % v/v). Similar to the bench-scale results, retention of ethanol (60 days, Figure 4b) was significantly longer than that of the tracer (4 days, curve not shown in Figure 4b). Mass recovery was calculated from aqueous effluent concentrations using the average flow rate over the 100-day duration of the experiment. Ethanol mass recovery was 70%, which is lower than that observed for both the bench-scale experiment (approximately 90%) and the previously reported E95 spill experiment that was conducted in the same pilot-scale tank (98%) (Cápiro et al. 2007). This lower recovery may be because of increased degradation and/or volatilization due to higher temperatures (summer for E100 vs. fall for the E95 spill), a capillary fringe injection (vs. a water table injection), and lower average seepage velocities (0.75 vs. 2.6 m/day).

Effluent hydrocarbon recoveries for m-xylene and TMB were both 8%. Mass recovered by dissolution from the source based on number of pore volumes passing through the source was expected to be similar to that for the bench-scale results. Therefore, the lower hydrocarbon recoveries vs. those observed in the bench-scale experiment were likely because of potential losses resulting from volatilization from the capillary zone and biodegradation that were not quantified. In addition, sorption onto the S.E. Texas sand could contribute to as much as 20% of the initial mass based on sorption estimates using the measured foc and pore water concentrations assumed to be in equilibrium with the initial NAPL source. Media cores were taken (day 125) downgradient of the emplaced source from the tank surface to approximately 10 cm below the water table at 0.25, 1.0, and 1.8 m downstream of the emplaced source. Concentrations were below detection (below 10 mg/kg) for all hydrocarbons except TMB and isooctane, and maximum concentrations for TMB and isooctane were 70 mg/kg, considerably lower than the maximum concentrations observed in the bench-scale experiment. However, during excavation following the experiment, Sudan-IV staining was observed on the outlet PVC pipes and on a single PVC well located 1 m downgradient along the centerline from the source. The vertical extent of the staining was 10 to 15 cm thick at the water table. These results are significant for they indicate that following the upgradient ethanol release, hydrocarbons were transported above the water table at a distance of nearly 2 m from the source region. Mechanisms for transport are likely to be a combination of solubilization followed by phase separation (Rixey et al. 2005) and mobilization (Falta 1998).

Pore Water Concentrations

Bench Scale

In the capillary zone, peak ethanol concentrations reached were 97% v/v at 30 cm (Table 4A, Figure 5a) and 87% v/v at 60 cm downgradient of the source (Table 4A, Figure 5b) following the release. The NAPL was likely removed mostly by dissolution; however, given the high ethanol concentrations in the capillary zone, NAPL mobilization was also possible near the ethanol front (Falta 1998). Significant enhancements of toluene, m-xylene, TMB, and isooctane (up to two and three orders of magnitude for TMB and isooctane, respectively) over ethanol-free solubilities in water were observed for 50 days until ethanol concentrations decreased to below 25% v/v. Relative increases of this magnitude at these ethanol concentrations are consistent with results achieved in batch equilibrium and column experiments (Heermann and Powers 1998; Rixey et al. 2005).

In contrast to results for the capillary zone, the peak ethanol concentrations observed in the saturated zone were only 2.1% v/v and 3.8% v/v for 15 and 45 cm from the source, respectively (Table 4A, Figures 5c and 5d). Given these ethanol levels, it is not surprising that hydrocarbon concentrations below the water table did not measurably increase compared with those prior to ethanol release, because cosolubilization is not significant for ethanol concentrations less than 5% (Rixey et al. 2005). For comparison, the chloride tracer test that preceded the ethanol release yielded significantly higher concentrations in the saturated zone (peak concentration = 4850 mg/L) vs. the capillary zone (peak concentration = 1250 mg/L) (Stafford 2007).

Pilot Scale

Table 4B shows maximum ethanol concentrations and Figure 6 shows representative hydrocarbon and ethanol concentration breakthrough curves for downgradient sampling points both above and below the water table. As in the bench-scale release, ethanol concentrations were much higher in the capillary zone than just 3 cm below the water table. In the capillary zone, ethanol concentrations reached a maximum of 20% v/v at 25 cm and 11% v/v at 45 cm down gradient of the source (Table 4B). The peak ethanol concentrations observed in the saturated zone were two orders of magnitude lower than those in the capillary zone, 0.08 % v/v at both 30 and 60 cm from the source (Table 4B and Figures 6c and 6d). Some elevations in concentrations of toluene, m-xylene, TMB, and isooctane occurred in the

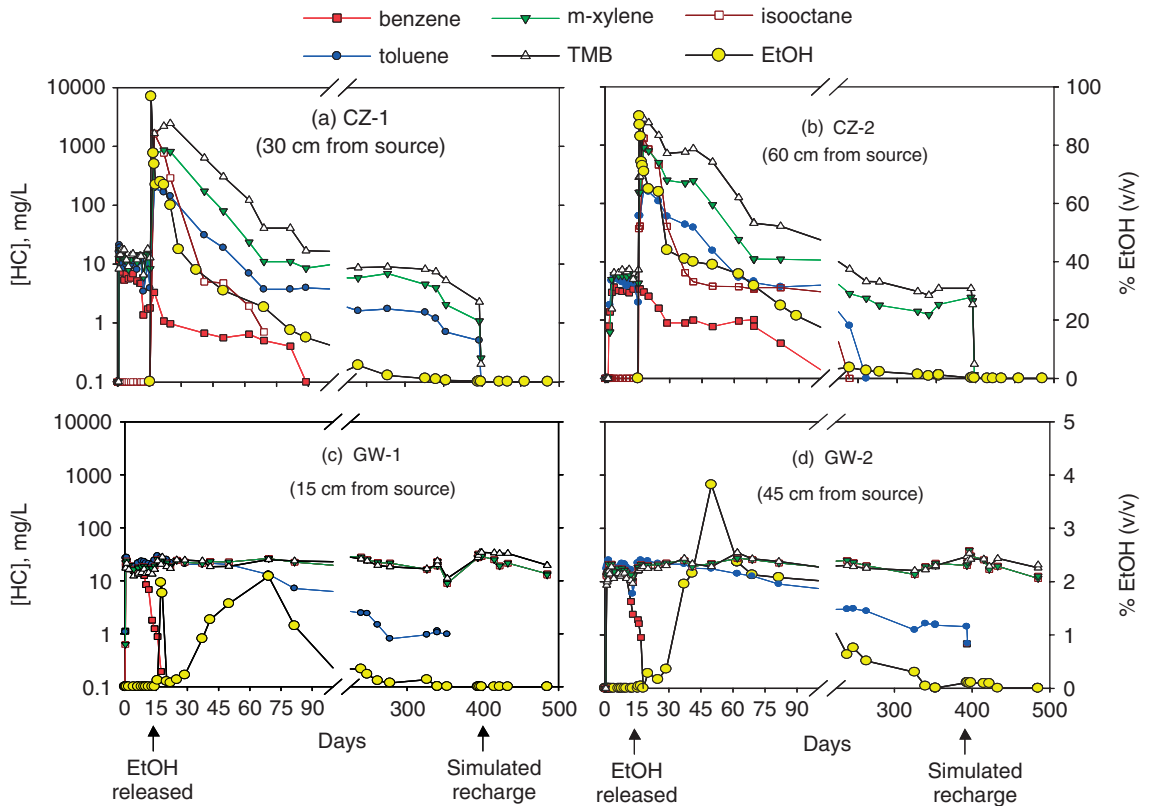

Figure 5. Two-dimensional bench-scale experiment. Breakthrough curves downgradient of the emplaced source. Ethanol was released on day 15.

Table 4
Maximum Ethanol Concentrations Measured in the Bench- and Pilot-Scale Releases
(SAT = Saturated Zone, CZ = Capillary Zone)

A. Bench-Scale Release

Distance from NAPL source		0.15 m	0.30 m	0.45 m	0.60 m
Zone		SAT	CZ	SAT	CZ
Max. conc.	(mg/L)	16,450	766,300	30,200	687,300
	(% v/v)	2.1	97	3.8	87

B. Pilot-Scale Release

Distance from NAPL source		0.15 m	0.25 m	0.30 m	0.45 m	0.60 m	0.75 m	1.2 m
Zone		SAT	CZ	SAT	CZ	SAT	CZ	SAT
Max. conc.	(mg/L)	240	158,000	600	84,270	590	158,000	280
	(% v/v)	0.03	20	0.08	11	0.08	20	0.04

capillary zone after ethanol was introduced, but they were much less pronounced than in the bench-scale release. The maximum concentrations observed in the capillary zone were 19 mg/L (benzene), 29 mg/L (toluene), 26 mg/L (m-xylene), and 39 mg/L (TMB) (Figures 6a and 6b). These concentrations are less than a factor of two higher than their respective effective water solubilities from the emplaced NAPL and are also consistent with previous equilibrium studies (Rixey et al. 2005) for the maximum level of ethanol (20% v/v) that was observed.

Below the water table, an increase in hydrocarbons was observed that corresponded to the increase in ethanol concentrations (Figures 6c and 6d). However, the maximum levels observed for all hydrocarbons were still below their effective water solubilities. Furthermore, a significant drop in dissolved oxygen was observed after the ethanol was introduced (Figure 6d). Therefore, it is likely that the increase in hydrocarbon concentrations was the result of a reduction in biodegradation due to preferential utilization of ethanol. It is also possible that cosolvency played a role, perhaps because of some NAPL mobilized in the capillary zone downstream that moved laterally to above the groundwater sampling point, but this was not observed in the bench-scale results where even higher ethanol concentrations

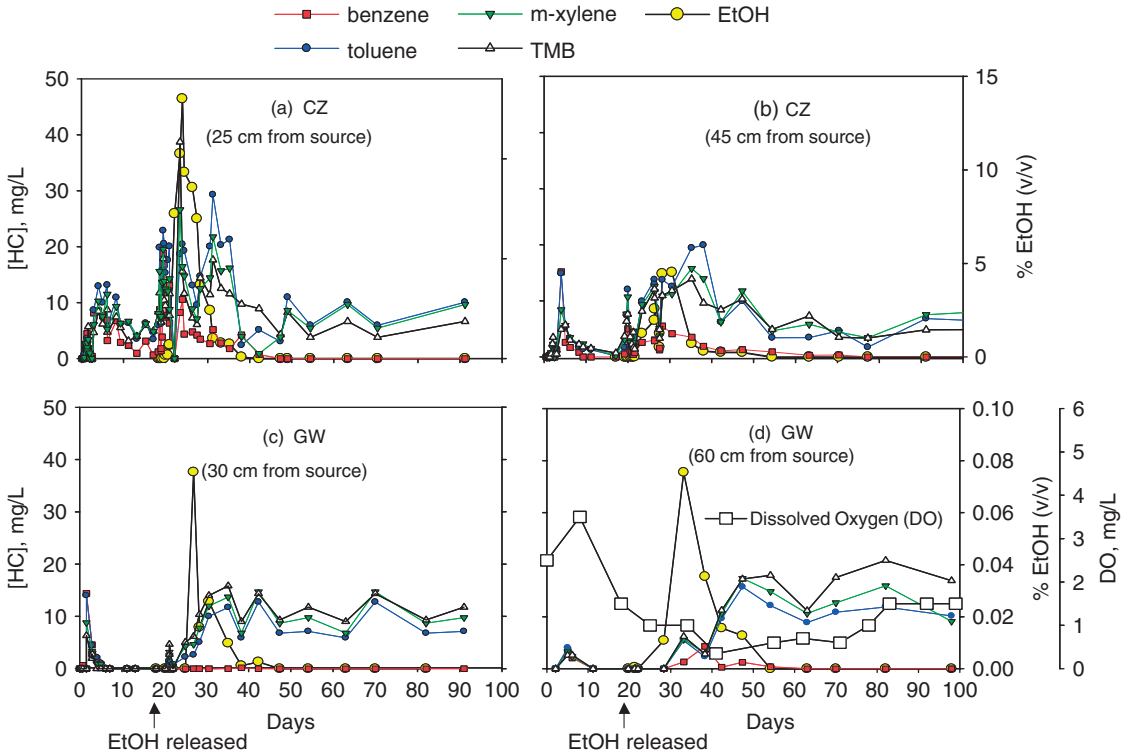

Figure 6. Pilot-scale experiment. Representative breakthrough curves downgradient of the emplaced source. Ethanol was released on day 18.

were measured. If the NAPL source is extended laterally, then concentrations measured in a ground water sampling point could increase further downstream of the original NAPL source due to mass transfer to ground water from NAPL above.

Mass Transfer of Ethanol from the Capillary Zone to below the Water Table

The low ethanol concentrations observed in the saturated zone relative to those in the capillary zone suggest that even though ethanol is completely miscible with water, ethanol concentrations in groundwater may be constrained by mass transfer limitations from the capillary to the saturated zone. To test this assumption, the following equation for vertical diffusion from a constant concentration source into a system with horizontal flow (Grathwohl 1998; Cussler 2003) was used:

$$C(x,z) = C_0 \mathrm{erfc}\left[\frac{z}{2\sqrt{D_z \, x/v_x}}\right] \quad (1)$$

where

$$D_z = \alpha_z v_x + \omega D_m \quad (2)$$

and C(x,z) is the concentration of ethanol at longitudinal distance-x (cm) from the ethanol release, point, and depth-z (cm) from the water table (g/cm^3), C_0 is the uniform ethanol concentration in the capillary zone (g/cm^3), D_z is the vertical dispersion coefficient of ethanol in pore water (cm^2/s), D_m is 0.84 × 10^{-5} (cm^2/s), the aqueous molecular diffusion coefficient for ethanol at infinite dilution at 25°C (Cussler 2003), v_x is the seepage velocity (cm/s), α_z is the vertical dispersivity (cm), and ω is a coefficient accounting for tortuosity (Bear 1972).

Ethanol concentrations in groundwater (normalized to the concentration in the capillary zone) for the bench- and pilot-scale experiment are shown in Figure 7. Data points from each release are from different locations at differing times during which the average concentrations at these points and in the capillary zone were relatively constant. Pseudo-steady-state groundwater concentration profiles were plotted that corresponded to source concentrations (C_0) of 40%, 5%, and 2% v/v for the bench-scale experiment and 20% and 10% v/v for the pilot-scale experiment. Best fits of the data for both experiments were obtained using a vertical dispersivity, α_z = 0.021 cm, and tortuosity, ω = 0.34. For the pilot-scale experiments, mechanical dispersion was controlling, whereas for the bench-scale experiments molecular diffusion was the major contribution to D_z. Thus, a unique set of values for ω and α_z was obtained from the curve fits to the data. For Figure 7, biodegradation was not considered.

Figure 7 indicates that the ethanol concentrations observed in ground water in both experiments can be explained in terms of advective-dispersive mass transfer from the capillary zone. It also demonstrates the important effect of seepage velocity and scale on concentrations of ethanol

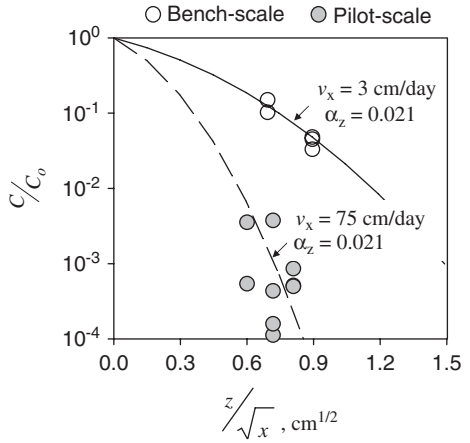

Figure 7. Comparison of maximum ethanol impacts to ground water in bench- and pilot-scale experiments. C_0 is the concentration at the capillary zone/water table interface.

in ground water. This figure provides a potentially simple way to conservatively estimate maximum concentrations of ethanol in ground water (in the absence of bioattenuation) that could be expected near a source for a given seepage velocity and spill size.

Conclusions

These results support previous studies showing that fuel ethanol releases will be largely confined to the capillary zone due to ethanol's buoyant properties. Additionally, we show that (1) in the absence of rapid water table fluctuations, mass transfer of ethanol from the capillary zone will determine the resulting ethanol concentrations in ground water and thus groundwater seepage velocity, dispersion, and position within and downgradient of the source will be important determinants of aqueous ethanol concentrations; and (2) pre-existing residual NAPL may be mobilized by ethanol in the capillary zone closer to the water table, which would increase hydrocarbon concentrations in neighboring ground water. These physical–chemical effects inform how to evaluate and monitor impacts from fuel ethanol releases and can be eventually considered with microbial effects and suitable transport models to determine the overall effect of ethanol spills on hydrocarbon plume dynamics.

Acknowledgments

This work was funded in part by the Texas Hazardous Waste Research Center and the American Petroleum Institute. The authors would also like to thank Andrea Zimmer, Ross Gordon, and Mark Measell for their assistance with tank preparation and sampling.

References

Abit, S.M., A. Amoozegar, M.J. Vepraskas, and C.P. Niewoehner. 2008. Solute transport in the capillary fringe and shallow groundwater: Field evaluation. *Vadose Zone Journal* 7: 890–898.

Bear, J. 1972. *Dynamics of Fluids in Porous Media*, 764. New York: Elsevier Publishing Company.

Cápiro, N.L., M.L.B. Da Silva, B.P. Stafford, W.G. Rixey, and P.J.J. Alvarez. 2008. Microbial response to a release of neat ethanol onto residual hydrocarbons in a pilot-scale aquifer tank. *Environmental Microbiology* 10, no. 9: 2236–2244.

Cápiro, N.L., B.P. Stafford, W.G. Rixey, P.B. Bedient, and P.J.J. Alvarez. 2007. Fuel-grade ethanol transport and impacts to groundwater in a pilot-scale aquifer tank. *Water Research* 41: 656–664.

Corseuil, H.X., B.I.A. Kaipper, and M. Fernandes. 2004. Cosolvency effect in subsurface systems contaminated with petroleum hydrocarbons and ethanol. *Water Research* 38: 1449–1456.

Cussler, E.L. 2003. *Diffusion: Mass Transfer in Fluid Systems*. Cambridge, UK: Cambridge University Press.

da Silva, M.L., and P.J.J. Alvarez. 2002. Effects of ethanol versus MTBE on benzene, toluene, ethylbenzene, and xylene natural attenuation in aquifer columns. *ASCE Journal of Environmental Engineering* 128: 862–867.

Deeb, R.A., J.O. Sharp, A. Stocking, S. McDonald, K.A. West, M. Laugier, P.J.J. Alvarez, M.C. Kavanaugh, and L. Alvarez-Cohen. 2002. Impact of ethanol on benzene plume lengths: Microbial and modeling studies. *ASCE Journal of Environmental Engineering* 128: 868–875.

Falta, R. 1998. Using phase diagrams to predict the performance of cosolvent floods for NAPL remediation. *Ground Water Monitoring and Remediation* 18: 94–102.

French, R., and P. Malone. 2005. Phase equilibria of ethanol fuel blends. *Fluid Phase Equilibria* 228: 27–40.

Gomez, D.E., P.C. de Blanc, W.G. Rixey, P.B. Bedient, and P.J.J. Alvarez. 2008. Modeling benzene plume elongation mechanisms exerted by ethanol using RT3D with a general substrate interaction module. *Water Resources Research* 44: W05405. doi:10.1029/2007WR006184.

Grathwohl, P. 1998. *Diffusion in Natural Porous Media: Contaminant Transport, Sorption/Desorption and Dissolution Kinetics*, 207. Boston, Massachusetts: Kluwer Publishing.

Grubb, D.G., and N. Sitar. 1999. Horizontal ethanol floods in clean, uniform, and layered sand packs under confined conditions. *Water Resources Research* 35, no. 11: 3291–3302.

Henry, E.J., and J.E. Smith. 2002. The effect of surface-active solutes on water flow and contaminant transport in variably saturated porous media with capillary zone effects. *Journal of Contaminant Hydrology* 56: 247–270.

Heermann, S.E., and S.E. Powers. 1998. Modeling the partitioning of BTEX in water-reformulated gasoline systems containing ethanol. *Journal of Contaminant Hydrology* 34: 315–341.

Jawitz, J.W., M.D. Annable, and P.S.C. Rao. 1998. Miscible fluid displacement stability in unconfined porous media: Two-dimensional flow experiments and simulations. *Journal of Contaminant Hydrology* 31: 211–230.

Lee, K.Y. 2008. Viscosity of high-alcohol content fuel blends with water: Subsurface contaminant transport implications. *Journal of Hazardous Materials*. doi:10.1016/j.jhazmat.2008.02.088

Lide, D.R, ed. 2005. *CRC Handbook of Chemistry and Physics*, 86th ed. Boca Raton, Florida: CRC Press Inc.

MacKay, D.M., N.R. De Sieyes, M.D. Einarson, K.P. Feris, A.A. Pappas, I.A. Wood, L. Jacobson, L.G. Justice, M.N. Noske, K.M. Scow, and J.T. Wilson. 2006. Impact of ethanol on the natural attenuation of benzene, toluene, and *o*-xylene in a normally sulfate-reducing aquifer. *Environmental Science and Technology* 40: 6123–6130.

McDowell, C.J., and S.E. Powers. 2003. Mechanisms affecting the infiltration and distribution of ethanol-blended gasoline in the vadose zone. *Environmental Science and Technology* 37: 1803–1810.

McDowell, C.J., T. Busheck, and S.E. Powers. 2003. Behavior of gasoline pools following a denatured ethanol spill. *Ground Water* 41: 746–757.

Molson, J.W., M. Mocanu, and J.F. Barker. 2008. Numerical analysis of buoyancy effects during dissolution and transport of oxygenated gasoline in groundwater. *Water Resources Research* 44: W07418. doi:10.1029/2007WR006337.

Molson, J.W., J.F. Barker, E.O. Frind, and M. Schirmer. 2002. Modeling the impact of ethanol on the persistence of benzene in gasoline-contaminated groundwater. *Water Resources Research* 38: 4-1–4-12.

Powers, S.E., C.S. Hunt, S.E. Heermann, H.X. Corseuil, D. Rice, and P.J.J. Alvarez. 2001a. The transport and fate of ethanol and BTEX in groundwater contaminated by gasohol. *Critical Reviews in Environmental Science and Technology* 31: 79–123.

Powers, S.E., D. Rice, B. Dooher, and P.J.J. Alvarez. 2001b. Will ethanol-blended gasoline affect groundwater quality? *Environmental Science and Technology* 35: 24A–30A.

Rao, P.S.C., M.D. Annable, R.K. Sillan, D. Dai, K. Hatfield, W.D. Graham, A.L. Wood, and C.G. Enfield. 1997. Field-scale evaluation of in situ cosolvent flushing for enhanced aquifer remediation. *Water Resources Research* 33: 2673–2686.

Rixey, W.G., X. He, and B.P. Stafford. 2005. The impact of gasohol and fuel-grade ethanol on BTX and other hydrocarbons in ground water: effect on concentrations near a source. American Petroleum Institute Technical Publication No. 23.

Rixey, W.G., and X. He. 2001. Dissolution characteristics of ethanol from NAPL sources and the impact on BTX groundwater concentrations. In *Conference on Petroleum Hydrocarbons and Organic Chemicals in Groundwater*, 41–52. Dublin, Ohio: Ground Water Publishing Company.

Silliman, S. E., B. Berkowitz, J. Simunek, and M. Th. van Genuchten. 2002. Fluid flow and solute migration within the capillary zone. *Ground Water* 40: 76-84.

Stafford, B.P. 2007. Impacts to ground water from releases of fuel grade ethanol: source behavior. PhD Dissertation. University of Houston.

Biographical Sketches

B.P. Stafford, *a corresponding author, received his Ph.D. from the Department of Civil and Environmental Engineering, University of Houston, Houston, Texas. He is currently with Shell Global Solutions (US) Inc., 3333 Hwy. 6 South, Houston, TX 77082; (281) 544-8320; brent.stafford@shell.com*

N.L. Cápiro *received her Ph.D. from the Department of Civil and Environmental Engineering, Rice University, Houston, Texas. She is currently with the School of Civil and Environmental Engineering, Georgia Institute of Technology, 311 Ferst Drive, Atlanta, GA 30332-0512; ncapiro@alumni.rice.edu*

P.J.J. Alvarez *is with the Department of Civil and Environmental Engineering, Rice University, 6100 Main St., MS-317, Houston, TX 77005; (713) 348-5903; alvarez@rice.edu*

W.G. Rixey, *also a corresponding author, is with the Department of Civil and Environmental Engineering, University of Houston, 4800 Calhoun Rd., Houston, TX 77204-4003; (713) 743-4279; wrixey@uh.edu*